Journal Pre-proof

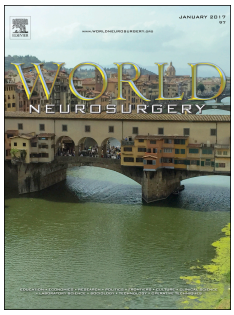

Hippocampal and orbitofrontal theta band coherence diminishes during conflict resolution

Austin M. Tang, MPH, Kuang-Hsuan Chen, PhD, Roberto Martin Del Campo-Vera, PhD, Rinu Sebastian, MS, Angad S. Gogia, BS, George Nune, MD, Charles Y. Liu, MD, PhD, Spencer Kellis, PhD, Brian Lee, MD, PhD

PII: S1878-8750(21)00563-5

DOI: https://doi.org/10.1016/j.wneu.2021.04.023

Reference: WNEU 17089

To appear in: *World Neurosurgery*

Received Date: 2 February 2021

Revised Date: 6 April 2021

Accepted Date: 6 April 2021

Please cite this article as: Tang AM, Chen K-H, Del Campo-Vera RM, Sebastian R, Gogia AS, Nune G, Liu CY, Kellis S, Lee B, Hippocampal and orbitofrontal theta band coherence diminishes during conflict resolution, *World Neurosurgery* (2021), doi: https://doi.org/10.1016/j.wneu.2021.04.023.

Full Title: Hippocampal and orbitofrontal theta band coherence diminishes during conflict resolution

Running Title: Theta coherence in conflict processing

Authors:

Austin M. Tang, MPH[a]
Kuang-Hsuan Chen, PhD[a]
Roberto Martin Del Campo-Vera, PhD[a]
Rinu Sebastian, MS[a]
Angad S. Gogia, BS[a]
George Nune, MD[b,c]
Charles Y. Liu, MD, PhD[a,c,d]
Spencer Kellis, PhD[a,c,d,e]
Brian Lee, MD, PhD[a,c,d]

Affiliations:

[a]Department of Neurological Surgery, Keck School of Medicine of USC, University of Southern California, Los Angeles, CA, United States
[b]Department of Neurology, Keck School of Medicine of USC, University of Southern California, Los Angeles, CA, United States
[c]USC Neurorestoration Center, Keck School of Medicine of USC, Los Angeles, CA, United States
[d]Department of Biology and Biological Engineering, California Institute of Technology, Pasadena, CA, United States
[e]Tianqiao and Chrissy Chen Brain-Machine Interface Center, Chen Institute for Neuroscience, California Institute of Technology, Pasadena, CA, United States

Corresponding Author:
Austin M. Tang, MPH
1200 N State Street, Suite 3300
Los Angeles, CA 90033
Email: austint@usc.edu
Phone: 323-226-7421
Office: 323-409-7422
Fax: 323-226-7833

Key Words
Coherence, theta, stroop, stereotactic electroencephalography hippocampus, orbitofrontal cortex, conflict processing

Full Title: Hippocampal and orbitofrontal theta band coherence diminishes during conflict resolution

Running Title: Theta coherence in conflict processing

Authors:

Austin M. Tang, MPH[a]
Kuang-Hsuan Chen, PhD[a]
Roberto Martin Del Campo-Vera, PhD[a]
Rinu Sebastian, MS[a]
Angad S. Gogia, BS[a]
George Nune, MD[b,c]
Charles Y. Liu, MD, PhD[a,c,d]
Spencer Kellis, PhD[a,c,d,e]
Brian Lee, MD, PhD[a,c,d]

Affiliations:

[a]Department of Neurological Surgery, Keck School of Medicine of USC, University of Southern California, Los Angeles, CA, United States
[b]Department of Neurology, Keck School of Medicine of USC, University of Southern California, Los Angeles, CA, United States
[c]USC Neurorestoration Center, Keck School of Medicine of USC, Los Angeles, CA, United States
[d]Department of Biology and Biological Engineering, California Institute of Technology, Pasadena, CA, United States
[e]Tianqiao and Chrissy Chen Brain-Machine Interface Center, Chen Institute for Neuroscience, California Institute of Technology, Pasadena, CA, United States

Corresponding Author:
Austin M. Tang, MPH
1200 N State Street, Suite 3300
Los Angeles, CA 90033
Email: austint@usc.edu
Phone: 323-226-7421
Office: 323-409-7422
Fax: 323-226-7833

Key Words
Coherence, theta, stroop, stereotactic electroencephalography hippocampus, orbitofrontal cortex, conflict processing

Abbreviations
Electroencephalography (EEG), magnetoencephalography (MEG), medial prefrontal cortex (mPFC), orbitofrontal cortex (OFC), local field potentials (LFPs), functional magnetic resonance imaging (fMRI), seizure onset zone (SOZ), computed tomography (CT), inter-trial interval (ITI), ventromedial prefrontal cortex (vmPFC)

Abstract

Objective

Coherence between the hippocampus and other brain structures has been shown with the theta frequency (3-8 Hz). Cortical decreases in theta coherence are thought to reflect response accuracy efficiency. However, the role of theta coherence during conflict resolution is poorly understood in non-cortical areas. In this study, coherence between the hippocampus and orbitofrontal cortex (OFC) was measured during a conflict resolution task. While both brain areas have been previously implicated in the Stroop task, their interactions are not well understood.

Methods

Nine patients were implanted with SEEG contacts in the hippocampus and OFC. Local field potential data were sampled throughout discrete phases of a Stroop task. Coherence was calculated for hippocampal and OFC contact pairs, and coherence spectrograms were constructed for congruent and incongruent conditions. Coherence changes during cue processing were identified using a non-parametric cluster-permutation t-test. Group analysis was conducted to compare overall theta coherence changes between conditions.

Results

In six out of nine patients, decreased theta coherence was observed only during the incongruent condition ($p < 0.05$). Congruent theta coherence did not change from baseline. Group analysis demonstrated lower theta coherence for the incongruent condition compared to the congruent condition ($p < 0.05$).

Conclusion

Theta coherence between the hippocampus and orbitofrontal cortex decreased during conflict. This finding supports existing theories that theta coherence desynchronization contributes to improved response accuracy and processing efficiency during conflict resolution. The underlying theta coherence observed between the hippocampus and OFC during conflict may be distinct from its previously observed role in memory.

Introduction

Brain oscillations have been observed using electroencephalography (EEG) in a wide gamut of brain functions such as cognitive processing, movement, and memory.[1-6] While oscillations may be studied within a single structure, they may also interact across different brain areas to guide behavior. This interaction can be measured and recorded in the brain as coherence.[7,8] Coherence has been well-studied in the context of memory formation and retrieval, particularly involving the hippocampus. Backus et al. (2016) used magnetoencephalography (MEG) data to observe synchronized coherence in the theta frequency band (4-8 Hz) between the hippocampus and medial prefrontal cortex (mPFC).[9] The authors hypothesized that initial theta oscillations within the hippocampus followed by coherence with the mPFC reflected dynamic memory encoding within the hippocampus and corresponding communication with the mPFC for higher level processing.[9] During memory recall, coherence between the hippocampus and the temporal-occipital cortex, amygdala, prefrontal cortex, and parietal lobe has also been observed within the theta band.[10-12] Outside of memory studies, coherence between the hippocampus and neocortex has been observed during behavioral inhibition using a task requiring numerical digit pattern detection.[13] In that study by Moore et al., it was hypothesized that as the neocortex played a role in cue detection, the hippocampus acted to reprogram motor output during cue resolution. Ekstrom et al. postulated that hippocampal-cortical synchronizations reflected connections between the hippocampus and areas more directly involved in higher level processing of sensorimotor and visual information, including those involved in conflict processing.[11] This study aims to characterize coherence patterns between the hippocampus and the orbitofrontal cortex, specifically in the context of conflict resolution.

While coherence increases have been emphasized during cognitive processes involved in memory and inhibitory functions, some studies highlight the phenomenon of decreased coherence during memory tasks, learning processes, or discordant presentation response. Gilboa and Moscovich et al. (2017) utilized a memory recall task to observe pre-stimulus sharp decreases in theta coherence between the ventromedial prefrontal cortex and infratemporal and lateral temporal cortices.[14] The authors found that this pre-stimulus desynchronization was correlated with response accuracy and activation of context-sensitive information. Some studies have hypothesized that high synchrony may reduce information coding, and that decreased inter-regional coherence may allow for expression of neural code more relevant to the changing task at hand.[15-18] Such hypotheses may be applied to learning processes and adaptation to new situations as well. Young and Shapiro et al. (2011) demonstrated coherence in theta band local field potentials (LFPs) between the orbitofrontal cortex (OFC) and hippocampus in rats carrying out a plus-maze task.[19] They found that high theta coherence values persisted during stable task performance, but fell when the task type was changed to force rats to adopt new behavior. This transient period of desynchronized activity in the hippocampus and the OFC may reflect the discordant predictions computed by the two structures.[19,20]

The previously cited studies attempt to characterize coherence using a variety of techniques in humans and rats, but human studies utilizing high temporal resolution recording techniques during tasks to demonstrate coherence changes during cognitive behaviors are limited. In the present study, a modified Stroop task was used to assess conflict resolution during measurement of coherence using intracranial electrodes via stereotactic electroencephalography (SEEG) between the hippocampus and OFC. The Stroop task is a well-known behavioral paradigm that utilizes color-word conflict scenarios, and has been widely studied in many brain

areas such as the hippocampus, and other cortical structures to characterize neural and behavioral reflections of conflict detection and resolution.[21,22]

While many brain areas have been implicated in Stroop-related conflict resolution, the OFC and hippocampus are known to be active in conflict scenarios. Increased hippocampal theta band activity in humans has been demonstrated both with SEEG recordings and functional magnetic resonance imaging (fMRI) during successful Stroop-related conflict processing.[23] However, the role of coherence in conflict resolution, particularly between the hippocampus and OFC, remains poorly understood. This study aims to utilize SEEG to characterize coherence in the hippocampus and OFC during a classic conflict resolution task. Based on prior findings of desynchronization in the theta band between the hippocampus and OFC during cognitive processing when presented with discordant scenarios, we hypothesize that theta band coherence between these two structures will decrease when participants face color-word conflict scenarios. Elucidating this relationship will improve understanding of the inter-structure connectivity involved with complex tasks, such as conflict processing, as well as glean further insight into the role of coherence in the brain.

Methods

Participants

Nine epileptic patients (2 female, age 20-62) participated in this study. All were implanted with intracranial depth electrodes for seizure localization and monitoring. Each patient was evaluated at a multidisciplinary pre-surgical planning meeting that included epileptologists, radiologists, and neurosurgeons to determine the number and placement site of electrodes. Participants provided written informed consent prior to participation in accordance with the University of Southern California Health Science Campus Institutional Review Board (HS-17-00554). Patients with implanted SEEG electrodes were monitored in the epilepsy monitoring unit (EMU) for approximately one week to allow for clinically indicated seizure localization. The number and location of SEEG electrodes were selected based on clinical requirements alone, and study activities were performed secondarily to clinical activities. During the outpatient clinical consultations, well before surgery, the patients were invited to participate in this study. Authorized research personnel discussed study activities, risks, benefits, and alternatives.[24] Patients could then choose whether to participate. Those who chose to participate provided written informed consent and were given a copy of the signed consent form. The study participants were informed that they could terminate the study at any time. Participants performed the Stroop task in a session of 30 minutes, including instruction, practice, and actual performance. After finishing a single session, participants were given a break for 10 minutes. Participants could then choose whether to have a second session, but no more than 2 sessions were performed per day. Patient enrollment occurred over the course of 18 months (March 2019 through August 2020). Patient characteristics, including seizure onset zone (SOZ), are presented in **Table 1**.

Electrodes and Recording Equipment

Two styles of AD-TECH (Oak Creek, WI) depth electrodes were implanted in the patients: one macro-only depth electrode with 8 or 10 macro ring-style contacts, and one macro-micro depth electrode with 6 macro and 10 micro contacts. Only data from the macro contacts were analyzed for this study. The macro-contact depth electrodes had a diameter of 1.1mm, and the macro-micro depth electrodes had a diameter of 1.3mm. Macro contacts on both styles of depth electrode were 1.57mm in length, and were spaced 5 mm apart center-to-center for macro-micro depth electrodes, 10mm for macro depth electrodes. The implanted electrode locations were confirmed with post-surgical computed tomography (CT) scans merged with pre-operative MRIs. **Figure 1** and **Figure 2** show merged CT/MRI images for a representative patient (P034) in the sagittal, coronal, transverse, and probe's-eye planes in the hippocampus and OFC, separately. The NeuroPort™ Neural Signal Processor (Blackrock Microsystems, Salt Lake City, UT) was used to record LFPs. LFP data was digitally sampled at both 30,000 samples/s and 2,000 samples/s with 16 bits and 250-nV resolution. Only the 2,000 samples/s data from the macro contacts located in gray matter in the hippocampus and OFC were used for analysis. Recording contacts were referenced to a quiet white matter contact as identified by a study clinical epileptologist on site during neural signal acquisition. **Table 2** details characteristics of the implanted electrodes in each patient, including the number of electrodes in the hippocampus and OFC. **Tables 3-1** and **3-2** summarize contact information, including the number of contacts in hippocampal and OFC gray matter for each patient. All patients except one (P045) had bilateral implantation.

Experimental Paradigm

We conducted a modified version of the classic Stroop task designed in the MATLAB® (2018b, The MathWorks, Inc., United States) with the Psychophysics toolbox.[25,26] In contrast to the classic Stroop task which used four colors: "Red", "Blue", "Green", and "Black", the modified Stroop task utilized in this study used eight colors: "Red", "Pink", "Yellow", "Green", "Blue", "Purple", "Brown", and "White." A touch-screen monitor was set up approximately one arm's-length away from the patient during performance of the tasks for comfortable viewing of the display. Color of the box or the texts showed on the monitor changed among different task conditions. The four task conditions are presented in **Figure 3**. In the first task condition, participants were asked to name the color of a 10 x 15cm solid-color block shown with a black background on the computer monitor. In the second condition, the name of a color was presented on the monitor in white-colored font (e.g. the word "Green" appeared on the monitor in white-colored font), and the patient was asked to read the text. In the third condition, the text was congruent with the font color (e.g. the word "Green" printed on the screen in green-colored font), and the patient was asked to name the color of the font. The fourth condition is similar to the third condition, except that the text was incongruent with the font color (e.g. the word "Green" printed on the screen in blue-colored font). A trial block was composed of 96 trials: the first and second conditions appeared 16 times each, whereas the third and fourth trial conditions were presented 32 times each. In the case of the third and fourth conditions, congruent and incongruent trials were pseudorandomly interleaved throughout the task to prevent anticipation of the trial conditions. An inter-trial interval (ITI) phase lasted for 1-2 seconds with a blank black background displayed shown on the monitor. Microphone data was used to record verbal responses and response times when available (eight out of nine patients). For the single patient (P032) without microphone data, study personnel manually pressed a key on the task computer keyboard to capture the timing of the response. Participants were asked to restrict movements such as eye and body movements to maintain within-patient controls during task administration.

Coherence Calculation

Every contact in target gray matter was used to calculate coherence values in the theta frequency band. Contact pairs, defined as a set of two contacts each from hippocampal and OFC gray matter, were used to calculate theta coherence values in every possible combination of eligible contacts within each patients. **Table 4** lists the number of available contact pairs in the ipsilateral condition (analyzed contacts in hippocampus and OFC cortex are in the same side) and contralateral condition for each patient.

Multi-taper cohereograms (time-bandwidth product: 5; number of leading tapers: 9; frequency range of interest: 0.1 to 150 Hz) were generated for each trial and each channel using the Chronux software package in MATLAB® (2018b, The MathWorks, Inc., United States).[27,28] The window and step sizes utilized in generating cohereograms were 0.8s and 0.05s, respectively. Trials with power greater than 1,000 μV^2 between 0.1-1Hz were excluded from analysis. Additionally, trials containing interictal spikes in the raw data, as identified by research personnel through manual review, were discarded. Two participants, P032 (12 congruent, 11 incongruent clean trials of 32 collected trials in each condition) and P033 (10 congruent, 9 incongruent clean trials of 64 collected trials in each condition), were excluded from analysis because few artifact-free trials remained. The number of artifact-free trials and total trials for congruent and incongruent trial condition for each patient are shown in **Table 4**. Each remaining artifact-free trial was trimmed to a 3.5 second stimulus-locked segment (1.5s pre-stimulus, 2s

post-stimulus) and a 2 second response-locked segment (1s pre-response, 1s post-response) before computing coherence. The details of calculating the z-scored coherence value, for each window in the set of moving windows, are as follows: first we calculated the multi-taper spectrum for two contacts. Next, the cross-spectrum of two contacts was calculated by multiplying the conjugate value of one channel's spectrum by the other channel's spectrum generated from the first step. This cross-spectrum value was the numerator of the formula for calculating the coherence value. The denominator was calculated as the square of the product of the two channel's spectrums. Finally, coherence values in the trimmed stimulus-locked and response-locked periods were z-scored per frequency bin using median and absolute median deviation coherence values computed during ITI period (0.8s – 0.2s pre-stimulus).

Statistical Analysis

A non-parametric cluster-permutation t-test was used to identify time-frequency points with statistically significant coherence change in theta (4-8 Hz) frequency band during the cue-processing period of the trial, compared to the baseline ITI phase. This statistical method was chosen because it has been previously used to control for family-wise Type I error without making assumptions on the underlying sample distribution in multi-channel time-frequency neural data.[29] First, the time period -0.8 seconds to -0.2 seconds prior to the cue was labelled as the resting phase (ITI phase) and the cue-processing period (i.e. post-stimulus, pre-response) was labelled as the "processing" phase for each trial. Next, for each channel, the order of these two labelled phases for all artifact-free trials was randomly shuffled. For each shuffle, a t-value and corresponding p-value, with a null hypothesis of no differences between coherence values during the ITI and cue-processing phase, were calculated for each data point. An uncorrected alpha-level of 0.05 was set as the threshold value for detection of time-frequency data points with significant coherence change with respect to the ITI phase. The use of an uncorrected alpha value is appropriate to control for family-wise Type I error because a whole grid of points, including time-frequency points, were compared with the same statistical test rather than testing for individual time-frequency points. Only the largest cluster containing the most significant data points was labelled, and the sum of all t-values in this cluster was calculated. This process was repeated 1,000 times to generate a representative null distribution of summed t-values for the cue-processing phase for each channel. The 95^{th} percentile of this distribution was used as the threshold value to determine significant clusters from unshuffled data in further testing. Finally, t- and p-values for each data point were calculated from unshuffled data, and the largest cluster of significant time-frequency points was identified as described above. The summed t-value from the largest cluster was compared to the 95^{th} percentile of the previous generated null distribution from shuffled data.

Group Analysis

Mean theta coherence values from one contact pair for each trial and patient in both congruent and incongruent conditions were calculated to conduct group analysis. A single pair of contacts was used for each patient to maintain equal weighting during group analysis. A mean theta coherence value was generated by averaging the theta coherence values within a 0.5 second window centered around the minimum theta coherence observed during the cue-processing period for both stimulus-locked segments and response-locked segments. Stimulus-locked refers to when the analyzed segments are aligned to the cue timestamps among trials; in contrast,

response-locked segments are aligned to the timestamp of the response. Any trial in which the stimulus and verbal response windows overlapped was excluded from group analysis.

The first group analysis is to investigate the main effect from the trial condition (congruent vs. incongruent), as well as hemisphere condition (ipsilateral vs. contralateral) on theta coherence by using the Two-way ANOVA. To maintain the same weighting from each patient and balanced design (equal number of observations for all possible condition combinations: 4 condition combinations calculated by 2 kinds of trial conditions (congruent and incongruent) multiplying 2 kinds of hemisphere conditions (ipsilateral and contralateral)) in the two-way ANOVA test, the smallest number of trials (TR_{min} = 25, from P047 contributed from the combination of congruent trial condition and ipsilateral condition) was applied in following random sampling process. For each patient and condition combination, we drew TR_{min} trials with replacement from mean theta coherence values calculated previously and combined them across analyzed patients. In this group analysis, P045 was excluded due to lack of data in the contralateral condition. Thus, a total of 6 analyzed patients were included in this group analysis. Of note, because of two electrode pairs available per hemisphere in P043 and P046, there were multiple possible combinations of trial condition and hemisphere. For example, in ipsilateral hemisphere condition, P043 showed 59 clean trials available in congruent trial condition from the right hippocampus and right OFC as well as the left hippocampus and left OFC. We treated them as the same ipsilateral hemisphere condition and combined them into one set of 118 trials for the ipsilateral hemisphere condition for P043. Thus, in the random sampling process, the TR_{min} samples were drawn with replacement from these 118 trials. Finally, there were 600 (4 condition combinations times 25 trials for 6 patients) trials in total across all patients and condition combinations.

The second group analysis aimed to assess association of the theta coherence change with either the processing of the cue information or the inhibition of the automatic response. The difference values of mean theta coherence values between incongruent and congruent trial conditions were computed separately for both stimulus-locked and response-locked segments in the ipsilateral hemisphere condition. The ipsilateral hemisphere condition was chosen because there were trials available from more patients (seven patients in the ipsilateral condition versus six in the contralateral condition). To maintain equivalence when combining trials across patients, we used a bootstrapped-sampling approach to compute the mean delta values for TRmin trials. We drew TR_{min} samples, with replacement (here, TR_{min} =18 was patient with the fewest number of trials), and computed the average of these trials. This process was repeated 1,000 times for each patient in both stimulus- and response-locked segments. These trial-averaged difference mean theta coherence values were combined across seven patients. A paired t-test was used to compare distributions of difference values for the stimulus- versus response-locked segments.

Behavioral Analysis

Verbal response times recorded by microphone were available in eight of the nine patients and were z-scored to the median and the median absolute deviation values of verbal response time for each patient. Trials with absolute z-scored values greater than three were labeled as outliers and excluded from behavior analysis. In the remaining clean trials, z-scored response times were used to compare in all four trial conditions using the following procedure: first, using a bootstrapped-sampling approach (n=1000) to maintain equivalence when combining trials across patients, we computed the mean z-scored response time for TR_{min} trials

(here, TR_{min} =16 is the fewest number of trials for a single patient), selected with replacement from the set of trials for each patient. Both the Kruskal-Wallis ANOVA and post-hoc tests were conducted to test significant differences in the mean z-scored verbal response time among the four task conditions.

Results

Coherence analysis

Figure 5 presents cohereograms for the analyzed seven patients according to the within-patient analysis results. Six out of seven patients showed significant decreases in theta coherence (cluster-permutation t-test, 100~400ms after cue appeared, $p< 0.05$) from the ITI period to the cue-processing phase in the incongruent trial condition. The red polygon plotted in **Figure 4** indicates the time and frequency window of significant change in coherence during successful incongruent trial condition. In these seven analyzed patients, P045 was the singular patient that showed increased theta coherence during the successful incongruent trial condition. **Table 4** details the contact pairs showing significantly decreased theta coherence for each patient. No significant change of theta coherence between the ITI phase and cue-processing in the congruent trial condition was observed.

One group analysis was conducted by applying a two-way ANOVA test to investigate the main effects of trial conditions (congruent or incongruent) and the hemisphere conditions (ipsilateral or contralateral), as well as the interaction effect between the trial conditions and hemisphere conditions on mean theta coherence changes during the cue-processing period. This analysis demonstrated a significant main effect from trial conditions, $F(1, 599) = 15.64$, $p < 0.001$, and no significant main effect from hemispheric conditions, $F(1, 599) = 0.003$, $p = 0.96$. No significant interaction effect was noted from the trial conditions and hemisphere conditions, $F(2, 599) = 2.42$, $p = 0.12$. Another group analysis was conducted to compare the calculated difference in mean theta coherence values (mean incongruent theta coherence minus mean congruent theta coherence) between stimulus-locked and response-locked segments. **Figure 5** displays bootstrap-sampled distributions of difference mean theta coherence values calculated from stimulus-locked and response-locked segments. Mean z-scores for difference mean theta coherence were -1.06 (stimulus-locked) and -0.32 (response-locked). This difference was determined to be statistically significant using a paired sample t-test (equal variances not assumed, $t(3999) = -59.81$, $p < 0.001$).

We also examined the theta coherence changes for failed trials in the incongruent condition. A total of 11 failure trials were available across seven analyzed patients. We used the same cluster-permutation t-test method applied for successful trials to evaluate the coherence changes during the failure trials of incongruent condition. **Figure 6** shows a trial-averaged cohereogram (n=8 artifact-free trials) and no significant coherence change was found in theta, beta, or low-gamma frequency bands.

Behavioral Analysis

For the eight out of nine patients with available microphone data, ANOVA testing revealed significant differences in the verbal response time across task conditions (Kruskal-Wallis, $p < 0.001$; **Figure 7**). A post-hoc test showed that each of the six pairwise comparisons exhibited significant differences (Tukey-Kramer multiple comparison test, $p < 0.001$).
No speed-accuracy tradeoff was noted in analysis. Only eleven failure trials occurred across the seven analyzed patients due to high task accuracy (average correct trials = 97%). All analyzed patients had at least one failure trial. For failure trials, mean response time was 1.17s (standard deviation = 0.39s); for successful trials, mean response time was 1.16s (standard deviation = 0.28s).

Discussion

In this study, we used a Stroop task to investigate the coherence changes between the OFC and the hippocampus in theta frequency band of local field potentials during conflict processing. Our results demonstrate a significant decline in theta coherence during the cue-processing period in the incongruent task condition when compared to baseline. No significant theta coherence changes were found in the congruent task condition, nor in failed incongruent task trials. The singular different factor between the incongruent and congruent condition is the consistency between the color of the font and the font itself. Hence, the observed decreased theta coherence in the post-cue, pre-response period during successful incongruent condition trials is likely specific for successful conflict processing. Furthermore, to examine the association between the observed decline in theta coherence with either the cue-processing or the inhibition response, we conducted the group analysis comparing the difference of mean theta coherence values between congruent and incongruent condition calculated separately in stimulus-locked and response-locked segments. The group analysis results showed that the difference in values of mean theta coherence is larger when signal segments are aligned to the cue compared to those calculated from the response-aligned segments. This suggested that the observed decreased theta coherence was more related to the processing of the stimulus information (a more cognitive role) than the inhibition of the automatic response (a more motor role). Our results indicate that when new scenarios contradict a prior learned association or semantic meaning (i.e. the word "GREEN" shown in color blue), a new association may need to be created to solve this new problem, which may be reflected in desynchronized activity between the two structures, which are OFC and hippocampus in this study. Similarly, in a study by Young et al., decreased theta coherence between the OFC and hippocampus was demonstrated in rats using a plus-maze task.[19] In their study, rats that needed to deviate from the normal path to seek food reward also exhibited decreased theta coherence between the OFC and hippocampus. However, this association between the two structures has not previously been noted in humans.

In humans, decreases in theta coherence have been noted in other brain areas using other paradigms. Gilboa and Moscovitch used EEG to observed decreases in coherence in the theta frequency band in patients with normal brain function during a personal familiarity task.[14] In that task, participants were asked to identify pictures of acquaintances, during which decreases in theta coherence were noted between the ventromedial prefrontal cortex (vmPFC) and infero- and lateral temporal brain areas. The authors found that these coherence drops were predictive of subsequent response accuracy in their study participants. In our study, theta coherence cues were only noted during conditions of color-word incongruency. Because the incongruent Stroop condition requires recall, it is possible that the observed decreases in hippocampal/OFC theta coherence represent an aspect of conflict processing related to memory recall and response accuracy, similar to the findings observed within the vmPFC by Gilboa and Moscovitch. This comparison is further supported by the similarity in studied brain areas in the two investigations, namely the commonality between vmPFC and OFC.[30]

Outside of this investigation's primary focus of coherence, a plurality of studies investigating the neural correlates of memory formation instead focus on increases in theta coherence.[9-11,15,16,31] Thus, both decreases and increases in theta coherence have been noted during memory formation, leading to the question of how both increases and decreases in coherence can contribute to cognitive function. In order to reconcile these findings, some hypothesize that decreased interregional coherence may allow for more efficient processing of neural code, particularly in abnormal situations.[32] In this hypothesis, situations requiring

increased demand for attention cause reduced coherence, leading to diminished variability among neurons responding to situation ahead of increased processing.[17,33,34] Young et al. observed increased theta coherence between the OFC and hippocampus in rats when already familiar with the correct path towards food reward in a maze task. In that study, the rats performing a maze task with changing solutions required adaptive behavior and resolution of conflicting previously learned memories. In contrast, a decline theta coherence was subsequently found when rats needed to deviate from the normal path due to a changed path with food reward. This decline in theta coherence may have distinct functional significance, reflecting a desynchronization for the brain regions to encode new task representations.

Several limitations should be noted in this investigation. First, the mechanism underlying interactions between these two areas during successful conflict processing is still unknown. For example, it remains possible that these two structures operate in parallel and perform independent computations, and subsequently ultimately guide the output system (i.e. motor system) to achieve the correct performance together. Conversely, one of these two structures may act on the other directly, which means a hierarchical mechanism could exist to achieve better performance. Continued research into these hypotheses is necessary to better understand these interactions between hippocampus and OFC. Another limitation is that only patients with refractory epilepsy were included as participants. Thus, as with all studies performed on epileptic patients, it remains a possibility that the observed results may be influenced by underlying epileptic neurophysiology. Although this specific limitation may reduce the generalizability to normal human neurophysiology, in the absence of active seizure events during the trial, it is unlikely that observed intracranial effects are significantly modulated by epileptic pathology.[35] Additionally, although many patients receive intracranial electrode placement, the specific placement sites of electrode contacts is ultimately governed by clinical necessity. Thus, because electrodes cannot be intentionally placed with the same coordinates in each patient, there exists heterogeneity in electrode number, contact site, and underlying demographic characteristics within the study population, limiting generalizability and the ability to attribute observed effects to precise hippocampal or orbitofrontal locations. Lastly, as applies to all SEEG studies, signals observed in the hippocampus or OFC may originate from other sites within the brain.

Conclusion

In this study, significant decreases in theta coherence between the hippocampus and orbitofrontal cortex in the setting of conflict resolution, particularly when observed in a stimulus-locked fashion. While previous thoughts have postulated that decreased coherence facilitates improved neural reliability in the facilitation of memory processing, we believe we are the first to propose that drops in theta coherence may also play a significant, albeit related, role in conflict processing when observed between brain structures critical for memory and cortical processing. Future research in other brain area combinations and with other task paradigms will enable deeper understanding of the relationship between conflict processing and neural coherence.

Funding

Funding: This work was supported by the National Center for Advancing Translational Science (NCATS) of the U.S. National Institutes of Health (KL2TR001854), the Tianqiao and Chrissy Chen Brain-Machine Interface Center at Caltech, the Meira and Shaul G. Massry Foundation, and the Taiwan-USC Postdoctoral Fellowship Program.

References

1. Artieda J, Alegre M, Valencia M, et al. [Brain oscillations: pathophysiological and potentially therapeutic role in some neurological and psychiatric diseases]. *An Sist Sanit Navar.* 2009;32 Suppl 3:45-60.
2. Karakaş S, Barry RJ. A brief historical perspective on the advent of brain oscillations in the biological and psychological disciplines. *Neurosci Biobehav Rev.* 2017;75:335-347.
3. Maguire MJ, Abel AD. What changes in neural oscillations can reveal about developmental cognitive neuroscience: language development as a case in point. *Dev Cogn Neurosci.* 2013;6:125-136.
4. Runge Y, Frings C, Tempel T, Pastötter B. Electrophysiological Correlates of Saving-Enhanced Memory: Exploring Similarities to List-Method Directed Forgetting. *Eur J Neurosci.* 2020.
5. Pastötter B, Bäuml KT. Distinct slow and fast cortical theta dynamics in episodic memory retrieval. *Neuroimage.* 2014;94:155-161.
6. Gogia AS, Martin Del Campo-Vera R, Chen KH, et al. Gamma-band modulation in the human amygdala during reaching movements. *Neurosurg Focus.* 2020;49(1):E4.
7. Buzsáki G, Chrobak JJ. Temporal structure in spatially organized neuronal ensembles: a role for interneuronal networks. *Curr Opin Neurobiol.* 1995;5(4):504-510.
8. Buzsáki G, Draguhn A. Neuronal oscillations in cortical networks. *Science.* 2004;304(5679):1926-1929.
9. Backus AR, Schoffelen JM, Szebényi S, Hanslmayr S, Doeller CF. Hippocampal-Prefrontal Theta Oscillations Support Memory Integration. *Curr Biol.* 2016;26(4):450-457.
10. Babiloni C, Vecchio F, Mirabella G, et al. Hippocampal, amygdala, and neocortical synchronization of theta rhythms is related to an immediate recall during rey auditory verbal learning test. *Hum Brain Mapp.* 2009;30(7):2077-2089.
11. Ekstrom AD, Watrous AJ. Multifaceted roles for low-frequency oscillations in bottom-up and top-down processing during navigation and memory. *Neuroimage.* 2014;85 Pt 2(0 2):667-677.
12. Thézé R, Guggisberg AG, Nahum L, Schnider A. Rapid memory stabilization by transient theta coherence in the human medial temporal lobe. *Hippocampus.* 2016;26(4):445-454.
13. Moore RA, Gale A, Morris PH, Forrester D. Theta phase locking across the neocortex reflects cortico-hippocampal recursive communication during goal conflict resolution. *Int J Psychophysiol.* 2006;60(3):260-273.
14. Gilboa A, Moscovitch M. Ventromedial prefrontal cortex generates pre-stimulus theta coherence desynchronization: A schema instantiation hypothesis. *Cortex.* 2017;87:16-30.
15. Hanslmayr S, Staresina BP, Bowman H. Oscillations and Episodic Memory: Addressing the Synchronization/Desynchronization Conundrum. *Trends in Neurosciences.* 2016;39(1):16-25.
16. Hanslmayr S, Staudigl T, Fellner MC. Oscillatory power decreases and long-term memory: the information via desynchronization hypothesis. *Front Hum Neurosci.* 2012;6:74.
17. Mitchell JF, Sundberg KA, Reynolds JH. Spatial attention decorrelates intrinsic activity fluctuations in macaque area V4. *Neuron.* 2009;63(6):879-888.

18. Schneidman E, Puchalla JL, Segev R, Harris RA, Bialek W, Berry MJ, 2nd. Synergy from silence in a combinatorial neural code. *J Neurosci.* 2011;31(44):15732-15741.
19. Young JJ, Shapiro ML. Dynamic coding of goal-directed paths by orbital prefrontal cortex. *J Neurosci.* 2011;31(16):5989-6000.
20. Wikenheiser AM, Schoenbaum G. Over the river, through the woods: cognitive maps in the hippocampus and orbitofrontal cortex. *Nat Rev Neurosci.* 2016;17(8):513-523.
21. Oehrn CR, Hanslmayr S, Fell J, et al. Neural communication patterns underlying conflict detection, resolution, and adaptation. *J Neurosci.* 2014;34(31):10438-10452.
22. Chen KH, Gogia AS, Tang A, et al. Beta-band modulation in the human hippocampus during a conflict response task. *J Neural Eng.* 2020.
23. Oehrn CR, Baumann C, Fell J, et al. Human Hippocampal Dynamics during Response Conflict. *Curr Biol.* 2015;25(17):2307-2313.
24. National Commission for the Protection of Human Subjects of Biomedical and Behavioral Research DoH, Education and Welfare (DHEW) (30 September 1978). The Belmont Report (PDF). Washington, DC: United States Government Printing Office.
25. Brainard DH. The Psychophysics Toolbox. *Spatial Vision.* 1997;10(4):433-436.
26. Pelli DG. The VideoToolbox software for visual psychophysics: transforming numbers into movies. *Spat Vis.* 1997;10(4):437-442.
27. Mitra P, Observed brain dynamics. 2007: Oxford University Press.
28. Townsend BR, Subasi E, Scherberger H. Grasp Movement Decoding from Premotor and Parietal Cortex. *The Journal of Neuroscience.* 2011;31(40):14386-14398.
29. Maris E, Oostenveld R. Nonparametric statistical testing of EEG- and MEG-data. *J Neurosci Methods.* 2007;164(1):177-190.
30. Hiser J, Koenigs M. The Multifaceted Role of the Ventromedial Prefrontal Cortex in Emotion, Decision Making, Social Cognition, and Psychopathology. *Biol Psychiatry.* 2018;83(8):638-647.
31. Fell J, Axmacher N. The role of phase synchronization in memory processes. *Nat Rev Neurosci.* 2011;12(2):105-118.
32. Hanslmayr S, Staresina BP, Bowman H. Oscillations and Episodic Memory: Addressing the Synchronization/Desynchronization Conundrum. *Trends Neurosci.* 2016;39(1):16-25.
33. Rajan K, Abbott LF, Sompolinsky H. Stimulus-dependent suppression of chaos in recurrent neural networks. *Phys Rev E Stat Nonlin Soft Matter Phys.* 2010;82(1 Pt 1):011903.
34. McAdams CJ, Maunsell JH. Effects of attention on orientation-tuning functions of single neurons in macaque cortical area V4. *J Neurosci.* 1999;19(1):431-441.
35. Long NM, Burke JF, Kahana MJ. Subsequent memory effect in intracranial and scalp EEG. *Neuroimage.* 2014;84:488-494.

Figure 1

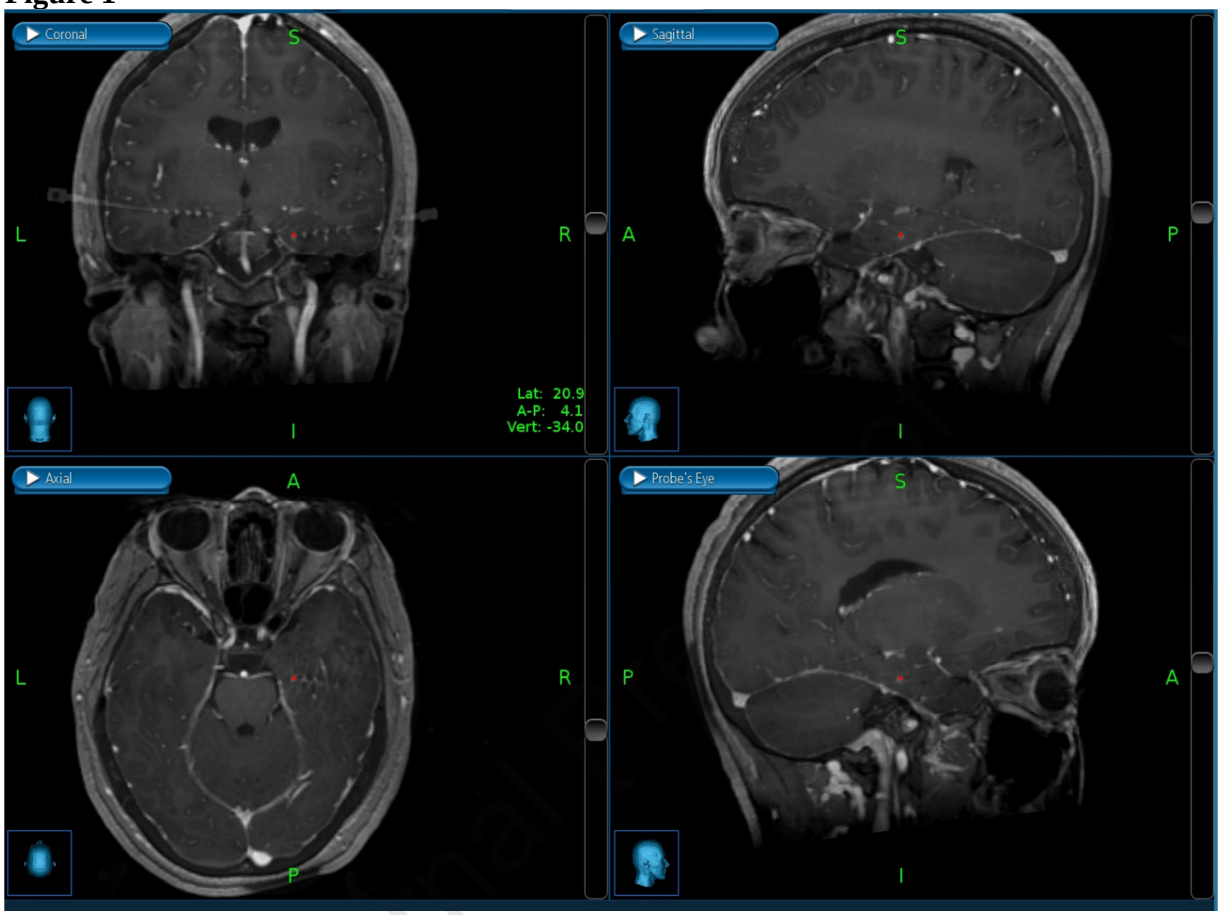

Figure 1. Merged CT/MRI image for electrode leads placed in the hippocampus in a representative patient (P034). Coronal, sagittal, axial, and probe's eye views are used in evaluation proper lead placement by using pre-operative and post-operative imaging.

Figure 2

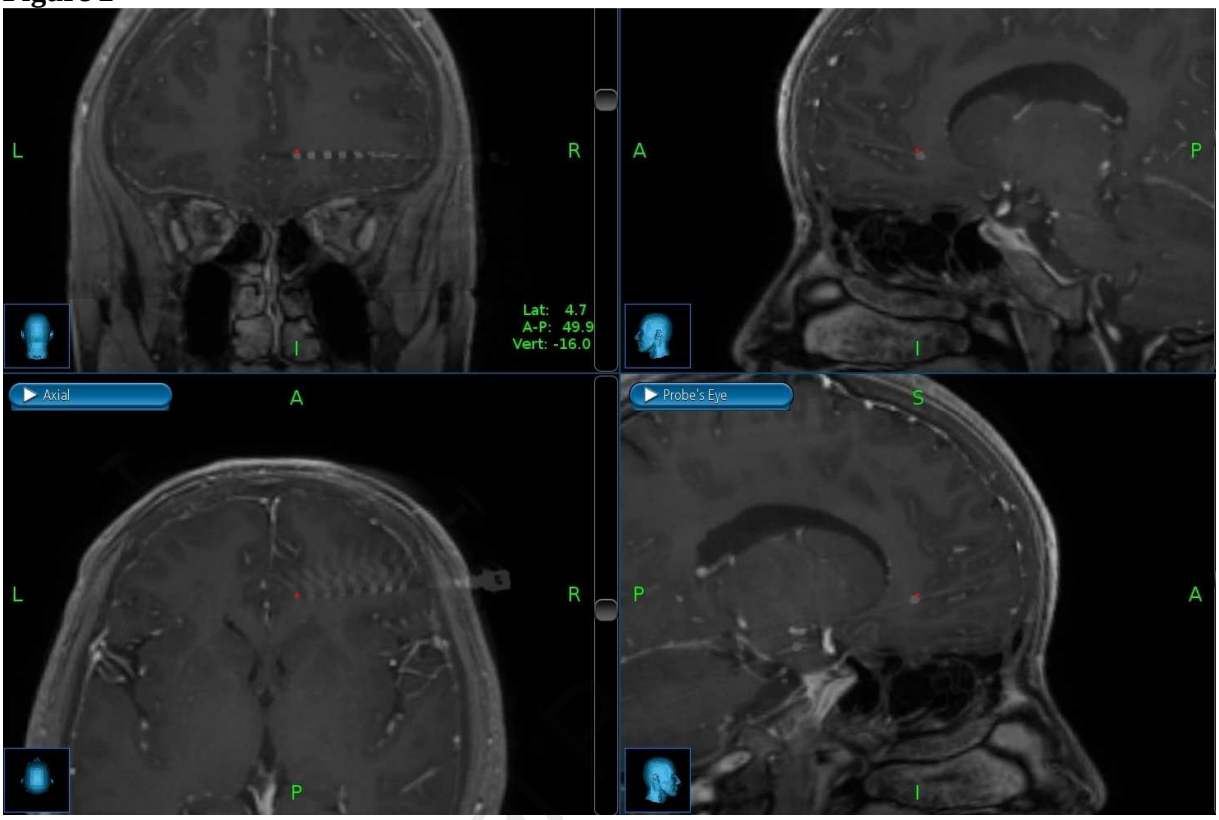

Figure 2. Merged CT/MRI image for electrode leads placed in the OFC in a representative patient (P034). Coronal, sagittal, axial, and probe's eye views are used in evaluation proper lead placement by using pre-operative and post-operative imaging.

Figure 3.

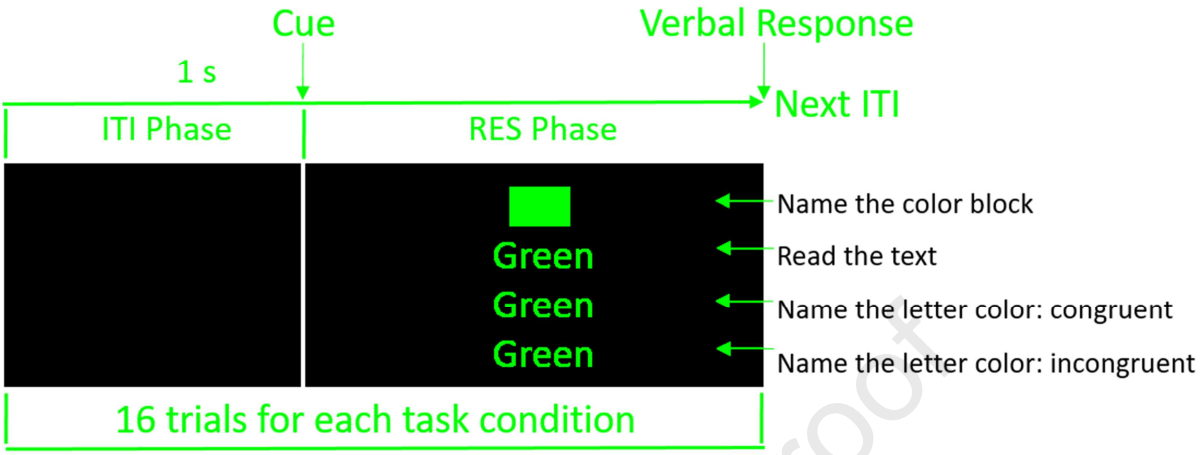

Figure 3. The modified Stroop task uses eight colors with four task conditions. The first condition requires naming of the color and the second requires reading neutral colored text. In the congruent condition, the text matches the color, while in the incongruent condition, the color does not match the text.

Figure 4.

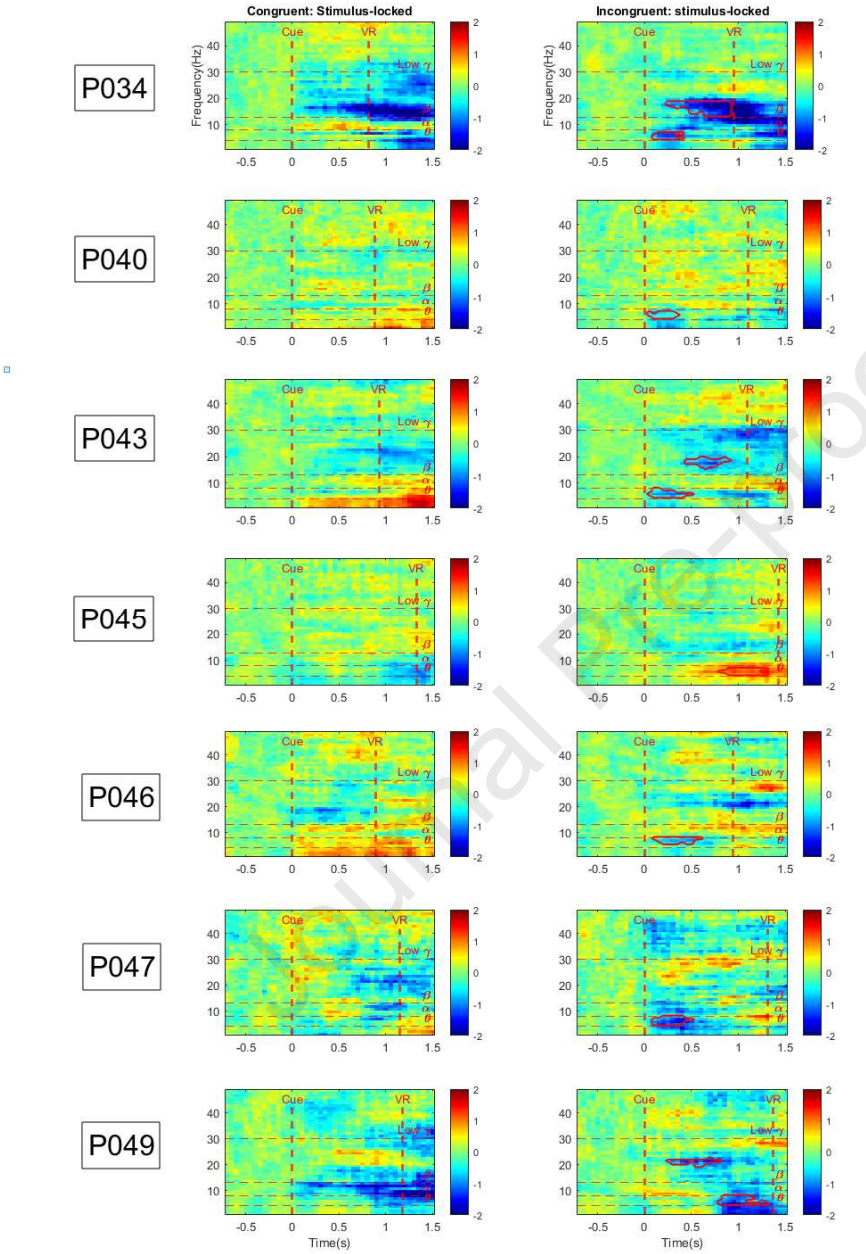

Figure 4. Time-frequency cohereograms for each study participant with stimulus-locked analysis. The first column depicts neural frequency bands measured during the congruent trial condition, while the second column depicts frequency bands during the incongruent trial condition. The overlaid red polygon encapsulates time-frequency periods of significant coherence change.

Figure 5. Distributions of mean theta coherence

Figure 5. Bootstrap-sampled distributions of delta averaged theta-coherence values (mean incongruent theta coherence minus mean congruent theta coherence) in stimulus-locked and response-locked analyses. Mean theta coherence for stimulus-locked segments was found to be significantly lower than that of response-locked segments.

Figure 6

Figure 6. Trial-averaged cohereograms for all incongruent condition failure trials (n=11) in both stimulus- and response-locked analyses. During failure trials, no significant changes in coherence were found in theta, beta, or low-gamma frequency bands by cluster-permutation t-testing.

Figure 7

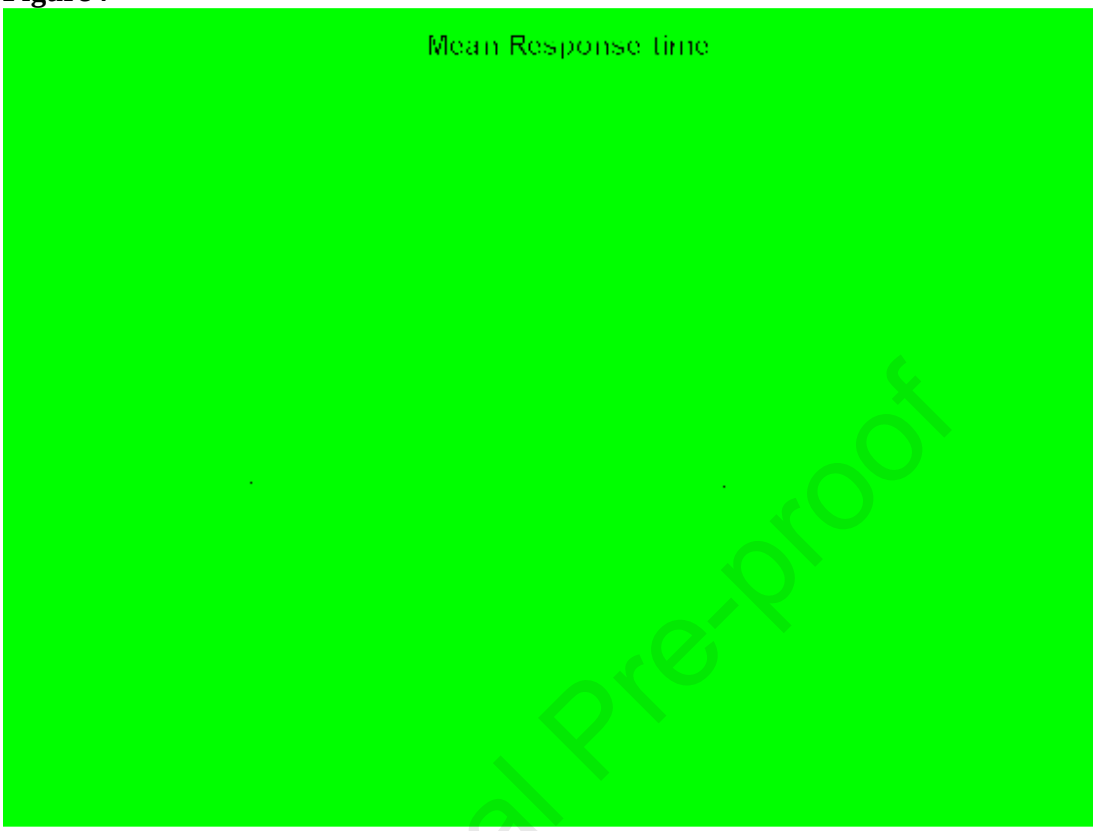

Figure 7. Boxplot depiction of mean value of the verbal response time in each task condition, among all patients. For each trial condition (color, text, congruent, incongruent), mean verbal response time was recorded via microphone available in eight patients. Distributions of mean response time were created using bootstrapped-sampling with replacement, and upon ANOVA testing were determined to be statistically significantly different in mean response time between trial conditions.

Table 1. Patient profiles

ID	Gender	Age	Handedness	Wada test	Seizure onset zone
32	M	62	Right	Left dominant	Right Orbitofrontal
33	F	26	Right	NA	Right Hippocampus
34	F	21	Right	NA	Right Hippocampus
40	M	23	Left	Left dominant	Right Amygdala
43	M	31	Right	Left dominant	Right Orbitofrontal Right Hippocampus
45	M	36	Right	NA	Right Anterior Cingulate Right Superior Temporal Right Premotor Cortex
46	M	32	Right	NA	Right Hippocampus Right Anterior Insula
47	M	40	Right	NA	Left Mesial Temporal Left Hippocampus Left Amygdala
49	M	27	Right	NA	Left Hippocampus

Table 1. Study participant characteristics, including seizure onset zone and Wada test results (when applicable).

Table 2. Information of implanted leads in hippocampus and orbitofrontal cortex

ID	# of implanted in hippocampus		# of implanted in orbitofrontal cortex	
32	Left	1 (Anterior)	Right	1 (Horizontal)
33	Right	2 (Anterior, Posterior)	Right	1 (Horizontal)
	Left	1 (Anterior)		
34	Right	2 (Anterior, Posterior)	Right	1 (Horizontal)
	Left	1 (Anterior)		
40	Right	2 (Anterior, Posterior)	Right	1 (Horizontal)
	Left	1 (Anterior)		
43	Right	1 (Anterior)	Right	3 (Vertical)
	Left	2 (Anterior, Posterior)	Left	2 (Horizontal & Vertical)
45	Right	1 (Anterior)	Right	1 (Horizontal)
46	Right	2 (Anterior, Posterior)	Right	2 (Horizontal & Vertical)
	Left	1 (Anterior)	Left	1 (Horizontal)
47	Left	2 (Anterior, Posterior)	Left	1 (Vertical)
49	Right	1 (Anterior)	Left	1 (Horizontal)
	Left	2 (Anterior, Posterior)		

Table 2. Characteristics of implanted electrodes in each patient in the hippocampus and orbitofrontal cortex.

Table 3-1. Summary of Contacts (Hippocampus)

ID	Hemisphere	Anterior		Posterior	
		Number of contacts in target gray matter	Total number of contacts per lead	Number of contacts in target gray matter	Total number of contacts per lead
P032	L	3	6	NA	NA
P033	R	3	6	1	6
	L	3	6	NA	NA
P034	R	3	6	0	6
	L	3	6	NA	NA
P040	R	1	6	0	6
	L	2	6	NA	NA
P043	R	2	6	NA	NA
	L	2	6	1	6
P045	R	2	6	NA	NA
P046	R	2	6	2	6
	L	2	6	NA	NA
P047	R	2	6	NA	NA
	L	3	6	0	6
P049	R	3	6	NA	NA
	L	2	6	0	6

Table 3-1. Number of contacts and leads in target hippocampal tissue for each patient, including anterior versus posterior localization.

Table 3-2. Summary for number of contacts used for analysis for each patient (Orbitofrontal cortex)

ID	Hemisphere	Number of contacts in target gray matter	Total number of contacts per lead
P032	R	4	10
P033	R	2	10
P034	R	3	8
P040	R	5	10
P043	R	3	10
	L	4	10
P045	R	2	8
P046	R	2	8
	L	2	8
P047	L	2	10
P049	L	4	10

Table 3-2. Number of contacts and leads in target hippocampal tissue for each patient, including anterior versus posterior localization.

Table 4. Summary of Contact Pairs Showing Significant Theta Coherence Change

Ipsilateral				
ID	Number of contact pair shows active theta coherence change	Number of contact pair	Number of artifact-free trials/Number of total trials	
			Congruent	Incongruent
P032*	NA	NA	12/32	11/32
P033*	0	6 (ROF†,RHH‡)	10/64	9/64
P034	4	9 (ROF,RHH)	58/64	57/64
P040	1	5 (ROF, RHH)	49/64	48/64
P043	2	6 (ROF, RHH)	59/64	60/64
	0	8 (LOF†, LHH‡)	59/64	60/64
P045	0	4 (ROF, RHH)	61/64	57/64
P046	0	4 (ROF, RHH)	55/64	54/64
	2	4 (LOF, LHH)	55/64	54/64
P047	1	6 (LOF, LHH)	25/32	27/32
P049	0	8 (LOF, LHH)	30/64	43/64
Contralateral				
ID	Number of contact pair show active theta coherence change	Number of contact pair	Number of artifact-free trials/Number of total trials	
			Congruent	Incongruent
P032*	0	12 (ROF, LHH)	Same as the numbers listed in ipsilateral information	
P033a	0	6 (ROF,LHH)		
P034	0	9 (ROF, LHH)		
P040	0	10 (ROF, LHH)		
P043	1	8 (ROF, LHH)		
	1	6 (LOF, RHH)		
P045	NA	NA		
P046	1	4 (ROF, LHH)		
	2	4 (LOF, RHH)		
P047	1	4 (LOF, RHH)		
P049	1	12 (LOF, RHH)		

Table 4. Summary of chosen contact pairs between the hippocampus and OFC for each patient. The total number of contact pairs and the number of contact pairs showing active theta coherence change are shown. Information on the number of trials that persisted for analysis after artifact removal are also displayed.

* P032 and P033 had few trials remaining after artifact removal, and were thus not included in analysis.

† Right (ROF) or left (LOF) orbitofrontal cortex

‡ Right (RHH) or left (LHH) hippocampal head

Figure 1

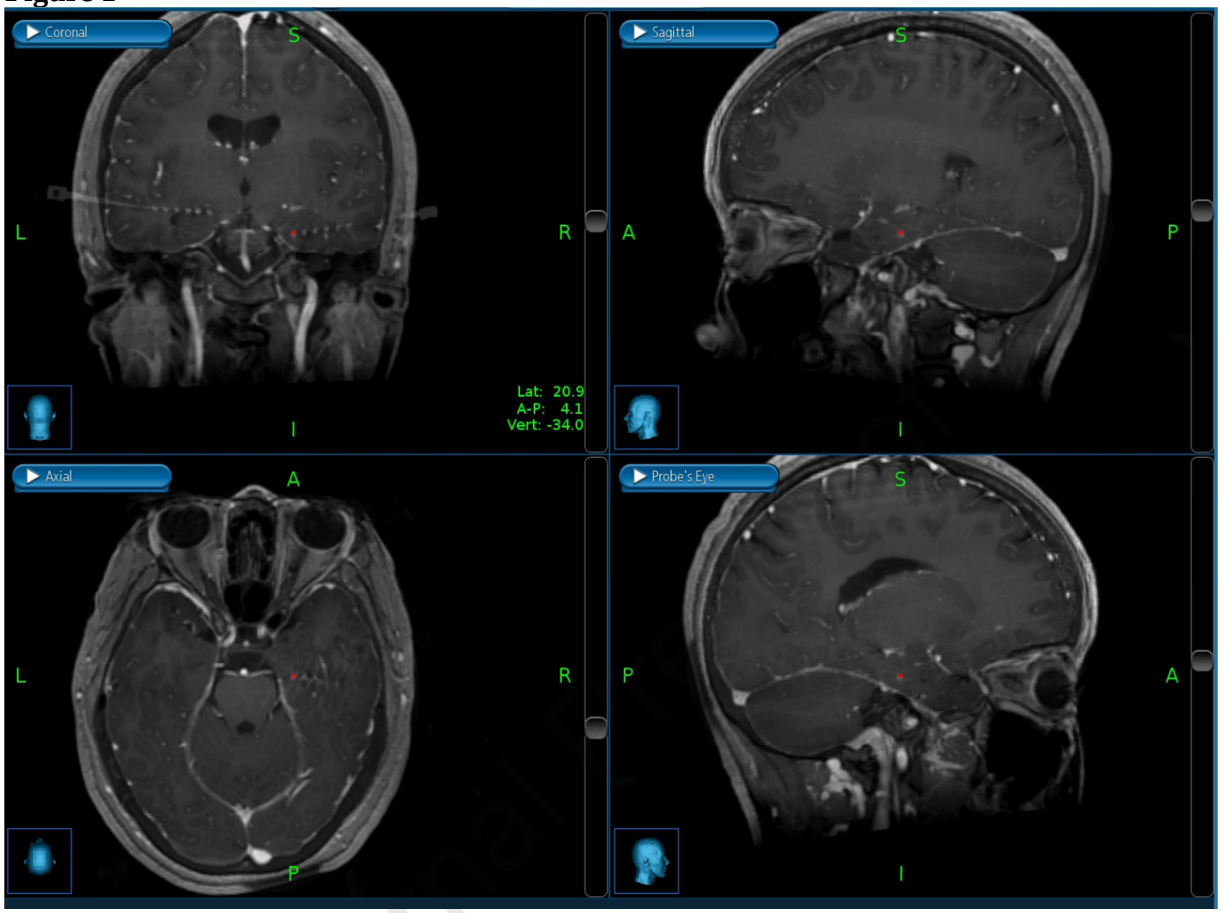

Figure 1. Merged CT/MRI image for electrode leads placed in the hippocampus in a representative patient (P034). Coronal, sagittal, axial, and probe's eye views are used in evaluation proper lead placement by using pre-operative and post-operative imaging.

Figure 2

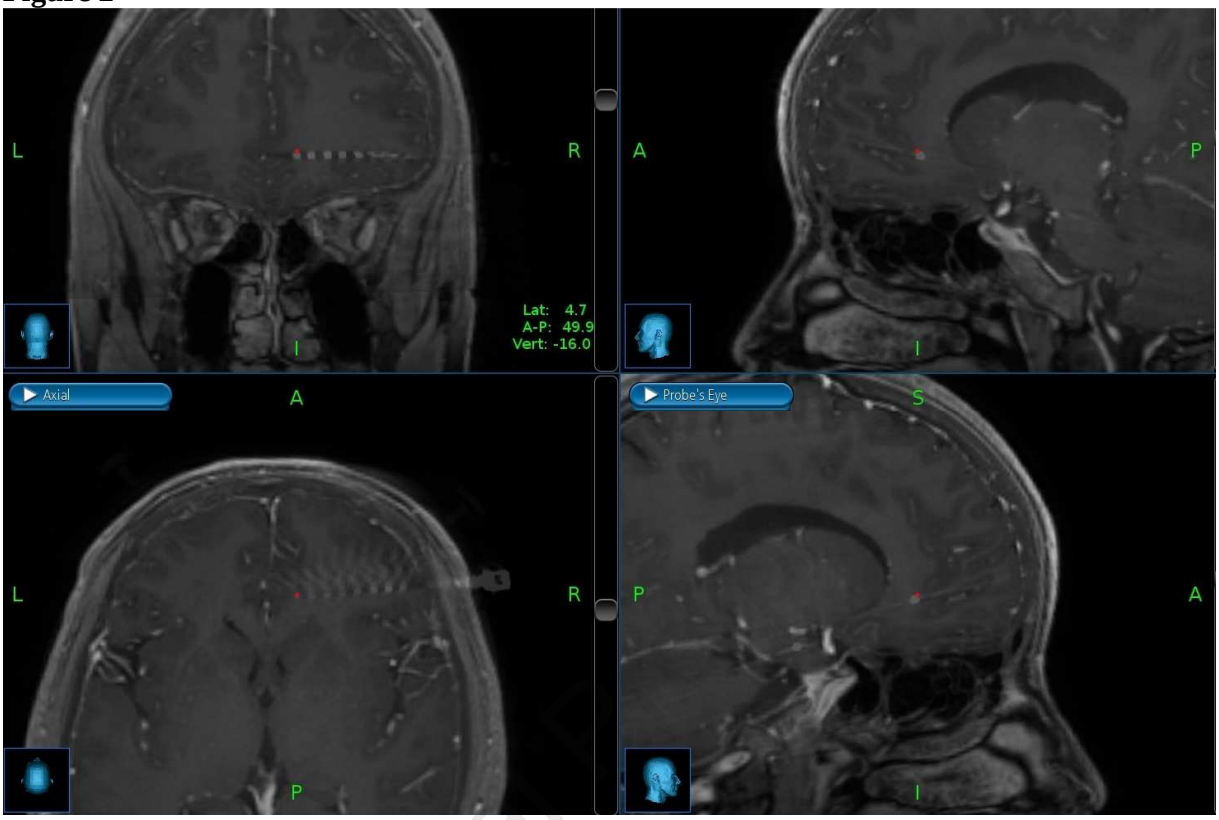

Figure 2. Merged CT/MRI image for electrode leads placed in the OFC in a representative patient (P034). Coronal, sagittal, axial, and probe's eye views are used in evaluation proper lead placement by using pre-operative and post-operative imaging.

Figure 3.

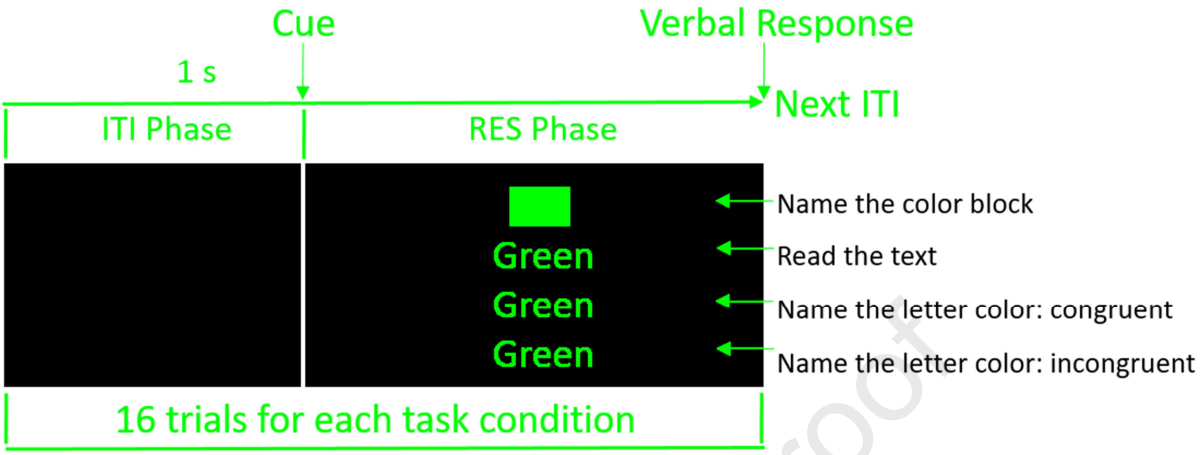

Figure 3. The modified Stroop task uses eight colors with four task conditions. The first condition requires naming of the color and the second requires reading neutral colored text. In the congruent condition, the text matches the color, while in the incongruent condition, the color does not match the text.

Figure 4.

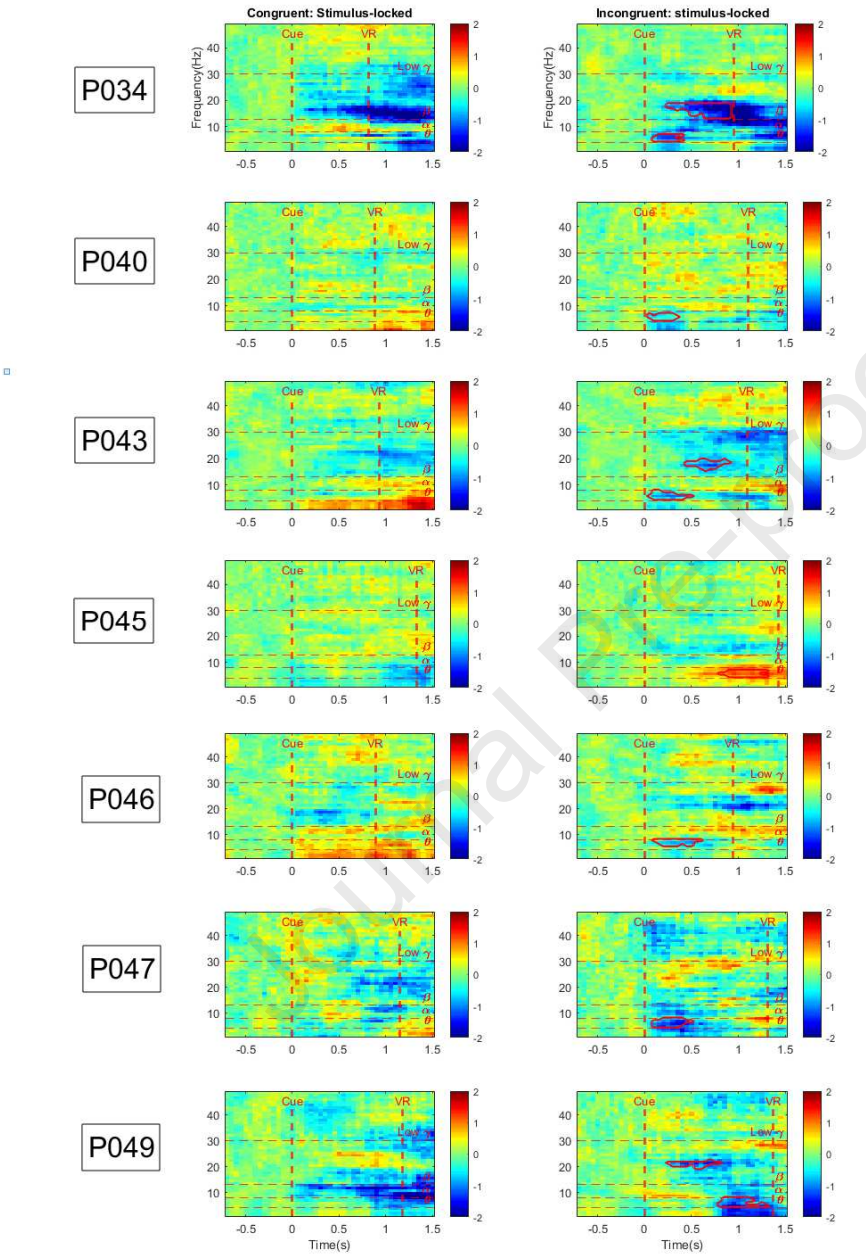

Figure 4. Time-frequency cohereograms for each study participant with stimulus-locked analysis. The first column depicts neural frequency bands measured during the congruent trial condition, while the second column depicts frequency bands during the incongruent trial condition. The overlaid red polygon encapsulates time-frequency periods of significant coherence change.

Figure 5. Distributions of mean theta coherence

Figure 5. Bootstrap-sampled distributions of delta averaged theta-coherence values (mean incongruent theta coherence minus mean congruent theta coherence) in stimulus-locked and response-locked analyses. Mean theta coherence for stimulus-locked segments was found to be significantly lower than that of response-locked segments.

Figure 6

Figure 6. Trial-averaged cohereograms for all incongruent condition failure trials (n=11) in both stimulus- and response-locked analyses. During failure trials, no significant changes in coherence were found in theta, beta, or low-gamma frequency bands by cluster-permutation t-testing.

Figure 7

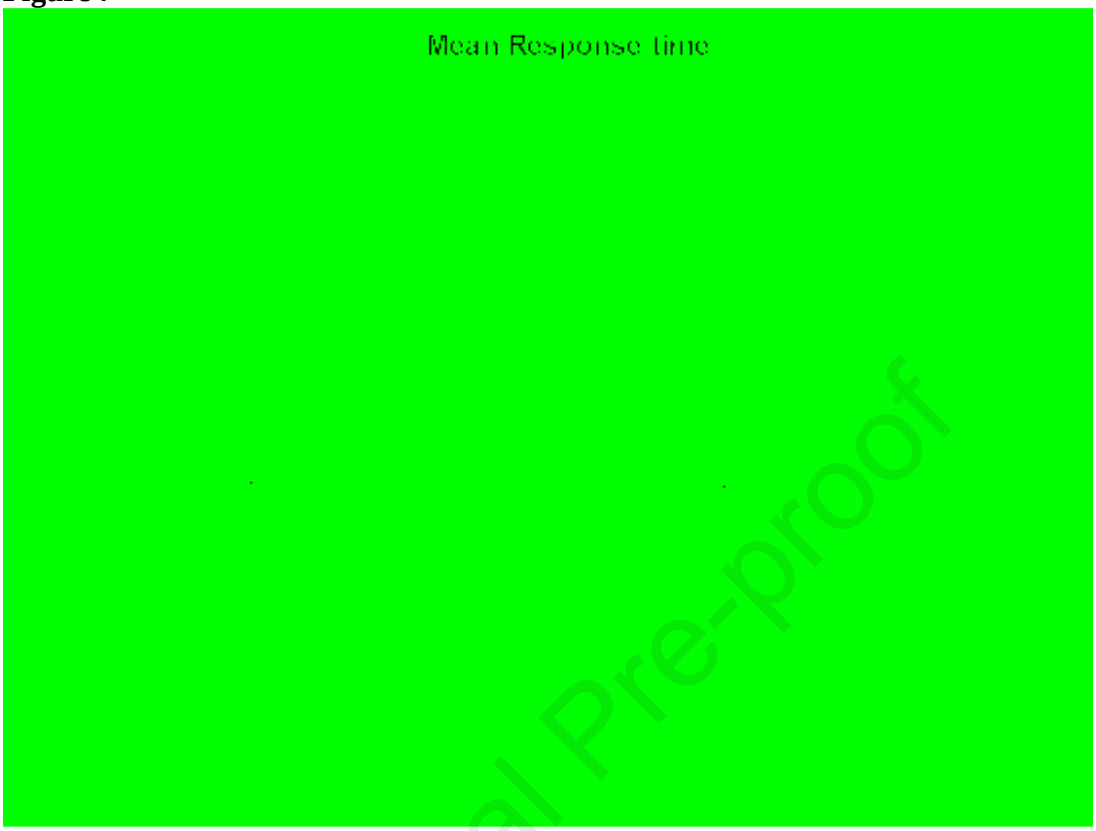

Figure 7. Boxplot depiction of mean value of the verbal response time in each task condition, among all patients. For each trial condition (color, text, congruent, incongruent), mean verbal response time was recorded via microphone available in eight patients. Distributions of mean response time were created using bootstrapped-sampling with replacement, and upon ANOVA testing were determined to be statistically significantly different in mean response time between trial conditions.

Abbreviations

Electroencephalography (EEG), magnetoencephalography (MEG), medial prefrontal cortex (mPFC), orbitofrontal cortex (OFC), local field potentials (LFPs), functional magnetic resonance imaging (fMRI), seizure onset zone (SOZ), computed tomography (CT), inter-trial interval (ITI), ventromedial prefrontal cortex (vmPFC)

Credit Author Statement:

Study Design: Austin Tang, Kuang-Hsuan Chen, Spencer Kellis, Brian Lee

Data Collection: Kuang-Hsuan Chen, Roberto Martin Del Campo-Vera, Rinu Sebastian, George Nune, Spencer Kellis, Brian Lee

Analysis: Kuang-Hsuan Chen, Rinu Sebastian, Spencer Kellis, Brian Lee

Manuscript Writing: Austin Tang, Kuang-Hsuan Chen, Spencer Kellis, Brian Lee

Internal Review: Austin Tang, Kuang-Hsuan Chen, Spencer Kellis, Brian Lee, Charles Liu, George Nune, Angad Gogia